Harnessing Demand Flexibility
in Electric Distribution Systems

Marie-Louise Arlt[*], David Chassin[†], Claudio Rivetta[‡], James Sweeney[§]

April 9, 2022

Abstract

The advent of decentralized energy resources allows distribution systems – the lower voltage levels of the electricity grid – to play an increasingly active role. In our work, we propose an integrated demand management system for residential distribution systems with a potential constraint on maximum load. Our proposal is characterized by an automated, real-time representation of customers' willingness-to-pay for dispatch by a smart home system and a market-based coordination of loads. We specify our approach for Heating, Ventilation, and Air Conditioning (HVAC) systems and show how customers can intuitively provide their preferences and how the smart home system automatically determines customers' willingness-to-pay. Even without market-based coordination, this design of the smart home system can immediately be implemented under real-time pricing. Moreover, we demonstrate the benefits of our approach in a case study of 437 houses in Austin, Texas, and estimate gains of more than 17,000 USD over one year, and significantly more in constrained systems. We further provide novel insights by analyzing the impacts of automation and real-time pricing among heterogeneous residential customers. We find that all customers contribute to the welfare gain and benefit in terms of consumer surplus but customers with large initial bills benefit over-proportionally, indicating potential re-distribution effects. Our work informs policy makers by illustrating the heterogeneous impacts of electricity pricing.

Keywords: Residential demand management, smart home systems, automation, distribution systems, local electricity markets

---

[*]Ludwig Maximilian University/SLAC, marie-louise.arlt@econ.lmu.de
[†]SLAC, dchassin@slac.stanford.edu
[‡]SLAC, rivetta@slac.stanford.edu
[§]Stanford University, jim.sweeney@stanford.edu

1   Introduction

The advent of decentralized energy resources such as solar energy as well as heat pumps, electric vehicles, or residential battery storage allows distribution systems – the lower voltage levels of the electricity grid – to play an increasingly active role in the efficient operations of power systems. In this work, we propose an integrated demand management system for residential distribution systems with a potential constraint on maximum load. Our integrated demand management is characterized by an automated, real-time representation of customers' willingness-to-pay for dispatch by a smart home system and a market-based coordination of loads.

Specifically, we suggest how the real-time willingness-to-pay for Heating, Ventilation, and Air Conditioning (HVAC) systems can be conceptualized in a consistent economic framework and operationalized in a smart home system. Previous work has relied on cost-minimizing strategies without economic trade-offs (e.g. [1, 2]), heuristics (e.g. [3, 4]), or non-automatable user input (e.g. [5, 6]). Other work like [7] uses similar assumptions but does not provide details on how to operationalize their strategy on a smart home system. In our work, however, we present a directly implementable and automatable design, from user input to dispatch.

Second, we further demonstrate in an extensive case study that our market-based demand management system can help to decrease the cost of distribution system operations and successfully manage a potential import constraint in real-time and in an automated way. Moreover, we are the first to provide evidence of the distributional consequences of automation under real-time pricing for HVAC systems, an appliance owned by a large share of the population. While previous work has demonstrated the aggregate benefits of real-time pricing and automation to manage load [e.g. 7, 8, 9], we analyze welfare and consumer surplus changes for individual customers with different characteristics, provide insight into the redistribution of consumer surplus between customers when switching from fixed to real-time pricing, and establish how welfare changes with price volatility. We are not aware of any study which would analyze welfare implications in similar detail.

Our work contributes to existing efforts to flexibilize demand and enable an efficient dispatch of resources [e.g. 10, 11, 12] as well as investment [e.g. 11, 13, 14, 15, 16]. Today, customers are mostly subject to fixed retail tariffs and do not efficiently respond to high real-time procurement cost of electricity [10]. Moreover, high demand in the residential distribution system can exhaust the import capacity from the overlying grid, damaging grid components or requiring the deployment of expensive reserve capacity [e.g. 4, 9].

Tariffs and programs such as Time-of-Use rates, real-time pricing, or critical peak pricing have shown to be generally effective in shaping residential demand and improve the efficiency of dispatch [e.g. 17, 18, 19]. Furthermore, dynamic pricing [e.g. 7, 20], local markets [e.g. 21, 3, 22, 23, 24, 5], and centralized dispatch optimization [e.g. 25, 26] have been proposed to manage residential appliances and local import constraints. For HVAC systems specifically, [7] present an approach for price-based control of a population of HVAC systems. These approaches to demand flexibilization allow to decrease system operations costs and, therefore, regulated retail tariffs and electricity bills for all households. In our paper, we choose a market-based approach which allows customers to express their preference for dispatch, is open to other appliances, and does not require access to private information for a centralized optimization.

With increasing shares of renewable energy and more volatile prices, automation has furthermore been recognized as key to access demand flexibility under fast-changing conditions [27, 9]. Although the technical literature proposes automated dispatch algorithms which minimize electricity cost – see [e.g. 1, 2] for HVAC systems or [e.g. 28, 29] for electric vehicles – the optimization disregards a trade-off with customer utility. Current designs of transactive systems enable automated bidding to local markets but the strategies are based on heuristics and their consistency with an economic framework is unclear [e.g. 21, 3, 4]. [7] consider a trade-off between utility and cost of customers for their price-based control of HVAC systems but they do not provide further details on the representation of (heterogeneous) preferences.

Extending this previous work, we suggest how the real-time willingness-to-pay for time-

interdependent electricity-based services can be conceptualized in a consistent economic framework and operationalized in a smart home system. We specify our approach for Heating, Ventilation, and Air Conditioning (HVAC) systems, a major residential and potentially flexible load, and demonstrate that it can be easily deployed: just as under a fixed retail rate, the setup of the HVAC system only requires two distinct inputs by the customer – the comfort temperature and a comfort preference – and we show that these parameters can be intuitively set through a slider in a smart home system. Importantly, our proposal for real-time dispatch can immediately be implemented in existing smart home systems and allow for automated response to a real-time price tariff. Smart home systems used for remote control and energy analysis, for instance, are becoming increasingly popular among customers [30, 31, 32, e.g.]. By implementing our dispatch strategy on such smart home systems, customers could avoid peak price events and high bills such as during the recent Texas energy crisis [e.g. 33].

Moreover, there is currently only limited insight on how residential demand management affects distribution systems, customers, and the distribution of consumer surplus between them. The literature on wholesale energy markets and transmission systems has broadly discussed the welfare gains enabled by load flexibility [e.g. 8, 11] and influenced policy making [34, 35, 36, 37]. However, it is unclear how such concepts can be transferred to residential distribution systems which are becoming increasingly important. Instead, previous work has focused on alternative performance indicators of residential demand management such as self-sufficiency [e.g. 5, 6] or successful capacity management in distribution systems [e.g. 3, 4]. [7] and [9] provide welfare estimates for their demand management approaches but do not enable a detailed analysis between customers. [38], however, highlight that the distributional consequences of time-dependent pricing can be substantial.

We extend previous work by demonstrating how our economic framework of customer preferences can be leveraged to study the welfare impact of automation and our demand management system in particular. In a case study of 437 houses in Austin, Texas, we estimate

welfare gains of more than 17,000 USD over one year and significantly more in systems with constrained import. Extending the level of detail of previous studies, we further find that all customers benefit from participation and that customers who contribute more to overall welfare also benefit more and even over-proportionally. However, the largest savings go to those who had high electricity bills in the first place. In our case study, high electricity bills are mainly driven by large floor sizes, indicating potential re-distribution effects between high- and low-income customers.

We proceed as follows: In Section 2, we derive a willingness-to-pay-based dispatch rule for time-interdependent electricity-based services and for HVAC operations in particular. In Section 3, we describe our market-based residential demand management system. Section 4 introduces our case study of 437 residential customers in Austin, Texas. We provide our results for customers and the retailer in Section 5, including changes of welfare, bills, and the distribution of consumer surplus. Section 6 concludes this paper by a brief summary, managerial and policy implications, as well as a research outlook.

2   Automating Customer Response to Real-Time Prices

In this section, we describe the customer's utility maximization problem and derive a real-time dispatch rule for implementation on a smart home system. First, we characterize the customer's willingness-to-pay for dispatch in a general model of time-interdependent electricity-based services (Section 2.1). Second, we specify our model for Heating, Ventilation, and Air Conditioning (HVAC) systems – a major and potentially flexible load in residential households – and derive a dispatch rule which is applicable under the assumption of limited information of the customer (Section 2.2).

2.1 General Customer Model

Residential customers operate electric appliances like HVAC systems, water heaters, or electric vehicles for their personal comfort. The dispatch of these appliances is usually discrete, i.e. $u \in \{0, 1\}$ (off/on), and influences the service level $x \in \mathbf{R}$. For instance, the dispatch of an HVAC system can provide the service of temperature control. The service level x is associated with the customer's utility $v(x)$, with $v'(x) \geq 0$ and $v''(x) \leq 0$. The cost of dispatch corresponds to $p \cdot P\Delta t$, where p is the per-unit cost of electricity and $P\Delta t$ the energy consumed during the dispatch. P is the power of the appliance and Δt the duration of dispatch. We assume that utility is linear in money.

The customer takes dispatch decisions at discrete points in time $t = 0, ..., T - 1$, with interval Δt. The dispatch of these appliances u_t usually impacts the service quality not only in the current period t but also in future periods. This time-interdependence is governed by a transition function $x_{t+1} = f(x_t, u_t, w_t)$. The future service level x_{t+1} depends on the previous state x_t, the dispatch decision u_t, and additional state information $w_t \in \mathcal{W}$. The state information w_t can capture weather conditions, for instance. In general, dispatch has a positive impact on the service level, i.e. $dx_{t+1}/du_t \geq 0$, and higher current service levels are associated with higher future service levels, i.e. $dx_{t+1}/dx_t \geq 0$. For example, both charging as well as a higher state-of-charge in t increase the state-of-charge of an electric vehicle in $t + 1$.

As the result of service level coupling over time, the customer faces an inter-temporal utility maximization problem over the optimization horizon T,

$$\max_{\mathbf{u_t}} \mathbb{E}\{\sum_{t=0}^{T-1}[v(x_t) - p_t P \Delta t u_t] + V_T(x_T)\} \tag{1}$$

$$\text{s.t. } x_{t+1} = f(x_t, u_t, w_t), \forall t \in \{0, ..., T-1\}$$

$$u_t, x_t \in \mathbf{C}^{load}, \forall t \in \{0, ..., T-1\}$$

$$p_{t+1} = g(p_t), w_{t+1} = h(w_t).$$

The problem is characterized by uncertainty with respect to future real-time prices p_t and state information w_t. Both follow a stochastic transition law, i.e. $p_{t+1} = g(p_t)$ and $w_{t+1} = h(w_t)$. In addition, dispatch and service quality can be subject to additional constraints $u_t, x_t \in \mathbf{C}^{load}$. These can include, for instance, the maximum state-of-charge of an electric vehicle battery or the maximum or minimum temperatures to be allowed for by an HVAC system. $V_T(x_T)$ captures the terminal utility, in particular the customer's utility changes after the end of the optimization horizon which were caused by dispatch decisions in $t < T$. Similar intertemporal optimization problems have been described by [7], among others.

The customer sequentially takes decisions about his dispatch. Given his expectations with respect to future prices and state variables, the customer chooses to dispatch in t whenever the expected value of dispatch exceeds the expected value of postponing dispatch, i.e.,

$$-p_t P \Delta t + \mathbb{E}\, V_{t+1}(x_{t+1}|u_t = 1) \geq \mathbb{E}\, V_{t+1}(x_{t+1}|u_t = 0), \tag{2}$$

where $V_{t+1}(x_{t+1})$ is the value function of the future state x_{t+1} and defined as follows,

$$V_{t+1}(x_{t+1}) := \max_{\mathbf{u_t}} \mathbb{E}\{\sum_{t'=t+1}^{T-1}[v(x_{t'}) - p_{t'} P \Delta t u_{t'}] + V_T(x_T)\}. \tag{3}$$

6

Symbol	Description	Symbol	Description
General model		*HVAC model*	
t	Time index	α	Comfort preference
T	Optimization horizon	θ_t	Internal temperature
$v(\cdot)$	Utility function	θ^{com}	Comfort temperature
$V_t(\cdot)$	Value function	θ^{out}	Outdoor temperature
b_t	Willingness to pay	β	Thermal house characteristics
x_t	Service quality	m	Operation mode (heating/cooling)
p_t	Local electricity price	γ_m	HVAC efficiency
P	Rated power of appliance	c_t^{WS}	Real-time cost of electricity
u_t	Dispatch	θ^{least}	Least favorable temperature in cycle
Δt	Market interval	θ^{most}	Most favorable temperature in cycle
$f(\cdot)$	Transition function	θ^{cycle}	Cycling temperature
$g(\cdot)$	Price transition law	$\Delta\theta_t$	Comfort gap
w_t	Global state	θ^{min}	Minimum temperature
$h(\cdot)$	Global state transition law	θ^{max}	Maximum temperature
$\mathbb{C}$	Constraints	$\Delta\theta_m^{max}$	Maximum comfort gap
$D_t(\cdot)$	Demand function		
c_t^{WS}	Wholesale market supply cost		

Table 1: Variables and parameters

We can use the definition of the value function to describe the customer's willingness-to-pay for dispatch, i.e. the maximum price, at which the customer would choose to dispatch. Determining the willingness-to-pay instead of optimizing dispatch directly has the key advantage that it easily extends to the participation of customers in other economic coordination mechanisms such as auctions. We will describe such a mechanism in Section 3.

Definition 2.1 *The willingness-to-pay b_t is defined as the price at which the customer is indifferent between current and future dispatch,*

$$b_t = \frac{V_{t+1}(x_{t+1}|u_t = 1) - V_{t+1}(x_{t+1}|u_t = 0)}{P\Delta t}.$$ (4)

The willingness-to-pay b_t depends on future prices. For example, higher future prices decrease the value of future operations, and more so, if the initial service level is low. There-

fore, an expected future price increase has a higher impact on the system with no dispatch in t than on the system with dispatch in t. As a result, the willingness-to-pay b_t described by Definition 2.1 increases with increasing expected future prices. The described interdependence of current dispatch and future prices contrasts the assumptions of other contributions on local demand management which do not consider demand and, therefore, the willingness-to-pay to be time-interdependent [e.g. 8, 39].

Dispatch occurs if the current price is less than or equal to the willingness-to-pay.

Definition 2.2 *The appliance-specific demand function $u_t(p_t)$ is defined as follows,*

$$u_t(p_t) = \begin{cases} 1, & for \quad p_t \leq b_t; \\ 0, & else. \end{cases} \tag{5}$$

2.2 HVAC System Model

The general model outlined above can be specified for time-interdependent dispatch for Heating, Ventilation, and Air Conditioning (HVAC) systems.

2.2.1 Model Specification

First, we model customer's utility from temperature control ('comfort') by a quadratic utility function [40],

$$v(\Delta\theta_t) = -\alpha\Delta\theta_t^2. \tag{6}$$

We define $\Delta\theta_t := |\theta_t - \theta^{com}|$, the deviation of the internal temperature θ_t from the customer-specific comfort temperature θ^{com}, as the 'comfort gap'. The negative comfort gap corresponds to the previously described service quality x_t, i.e. $x_t := -\Delta\theta_t$. The customer's utility level reaches its maximum if the internal equals the customer's comfort temperature, i.e. $\theta_t = \theta^{com}$. We normalize the maximum utility level to zero. Furthermore, utility decreases

8

with an increasing comfort gap, i.e. $\frac{dv(\Delta\theta_t)}{d\Delta\theta_t} < 0$, and more so at larger temperature devia-tions, i.e. $\frac{d^2v(\Delta\theta_t)}{d\Delta\theta_t^2} < 0$. As an additional constraint, we require that the internal temperature θ_t stays within a given temperature band, i.e. $\theta^{min} \leq \theta_t \leq \theta^{max}$.

Comfort is furthermore scaled by the comfort preference $\alpha \in \mathbf{R}_0^+$ which is customer-specific. Customers with a higher comfort preference α experience more severe comfort deterioration for a given comfort gap than customers with lower values of α, i.e. $dv/d\alpha < 0$. For $\alpha = 0$, customers are temperature-insensitive while customers with $\alpha \to \infty$ do not tolerate any temperature deviations. The latter could be the case for customers with medical conditions, for instance.

Second, modifying [41], we specify the transition function $\theta_{t+1} = f(\theta_t, u_t, \theta_t^{out})$ by the following equation,

$$\theta_{t+1} = \beta\theta_t + (1 - \beta)\theta_t^{out} + m\gamma_m P_m \Delta t u_t. \tag{7}$$

If the HVAC system is not operated ($u_t = 0$), the internal temperature θ_t converges to the outdoor temperature θ_t^{out}. θ_t^{out} specifies the state variable w_t of the general problem. The speed of convergence is determined by β which represents the thermal properties of the house. Higher β are associated with larger thermal inertia of the house, e.g. because of better insulation, and slow down the speed of convergence to the outdoor temperature θ_t^{out}. If the HVAC system is operated ($u_t = 1$), temperature convergence can be reversed. For $m = -1$, the HVAC system is in cooling mode and decreases the internal temperature; for $m = 1$, it is in heating mode and increases the internal temperature. γ_m indicates the efficiency of the HVAC system, depending on its operating mode $m \in \{-1, 1\}$.

As a final constraint and in line with real-world operational conditions of HVAC systems, we require $u_t \in \{0, 1\}$, i.e. the HVAC system can either operate at full power P_m or be idle. Therefore, HVAC systems cannot keep the internal temperature exactly at a desired level but only *on average* within a cycle. A cycle usually consists of a period during which the HVAC system operates and a number of sequential periods during which the HVAC does not operate. During the on period, the temperature changes from the least favorable temperature θ^{least} to

the most favorable temperature θ^{most}. During the off period, the temperature deteriorates from θ^{most} to θ^{least}, and the cycle restarts. Consequently, the temperature is controlled around the temperature level $\theta^{cycle} = (\theta^{most} + \theta^{least})/2$.

2.2.2 Willingness-to-Pay-Based Function

In the following, we derive the customer's willingness-to-pay-based dispatch function for HVAC dispatch. Such a function can be implemented on the customer's smart home energy system, a local controller which automatically dispatches devices given the customer's preferences. Automation has shown to increase price-based load response by removing the requirement for customers' attention to changing prices, see e.g. [27] and [9].

We consider it a design requirement for the dispatch function that it is easy to compute while reasonably reflecting the customer's trade-off between cost and comfort. Importantly, retail customers usually do not have sophisticated information about future prices or outside temperatures. Therefore, we design the smart home system to act myopically, i.e. based on the assumption that price and temperature levels stay constant over time or $\mathbb{E} \, p_{t+1} = \mathbb{E} \, g(p_t) = p_t = p$ and $\mathbb{E} \, \theta_{t+1}^{out} = \mathbb{E} \, h(\theta_t^{out}) = \theta_t^{out} = \theta^{out}$. However, we expect myopicity to have only minor impact on customer welfare: temperature degradation is relatively fast and the potential to take advantage of long-term price trends is therefore limited.

Given these assumptions, we can re-define our problem to the maximization of average utility under average dispatch $u := \frac{1}{T} \sum_{t=0}^{T-1} u_t \in [0, 1]$ ('duty cycle'). Then, the optimization problem simplifies as follows,

$$\max_{u}[v(\Delta\theta) - pP\Delta tu)] \tag{8}$$

Optimization and substitution reveal the customer's willingness-to-pay for comfort.

Theorem 2.1 (Willingness-to-Pay for Comfort.) *The willingness-to-pay to maintain*

an average comfort gap $\Delta\theta$ can be described by,

$$b = \begin{cases} \frac{2\alpha\gamma_m}{1-\beta}\Delta\theta, & for \quad \Delta\theta \leq \Delta\theta_m^{max}; \\ \infty, & else. \end{cases} \tag{9}$$

$\Delta\theta_m^{max}$ *is defined as the maximum average comfort gap, given θ^{min} and θ^{max}. A detailed derivation of this and the following theoretical results can be found in Section 7 in the appendix.*

We now describe the mechanics of price-based HVAC dispatch in discrete time, instead of *on average*. At time t, the house has an internal temperature of θ_t. Switching on the HVAC system would start a new cycle, with $\theta^{least} = \theta_t$ and $\theta^{most} = f(\theta_t, u_t = 1, \theta_t^{out})$ and a new temperature level of $\theta^{cycle} = (\theta_t + f(\theta_t, u_t = 1, \theta_t^{out}))/2$. We can apply Theorem 2.1 to determine the willingness-to-pay b_t for the associated comfort level $\Delta\theta$. If the willingness-to-pay b_t is equal to or exceeds the price level p, the HVAC system is dispatched, i.e. $u_t = 1$, and the internal temperature will be controlled around θ^{cycle}. If $b_t < p$, the HVAC system will not be dispatched as a control around θ^{cycle} would be too comfortable given the current price level p.

For a given constant price level p, we can furthermore derive the optimal comfort level $\Delta\theta^*$ and the optimal average dispatch u^*.

Proposition 2.2 (Optimal Comfort Gap.) *The optimal price-dependent comfort gap can be described by,*

$$\Delta\theta^* = \min\{\frac{1-\beta}{2\alpha\gamma_m}p, \Delta\theta_m^{max}\}. \tag{10}$$

Proposition 2.2 shows that the comfort gap would be zero if the cost of electricity was zero. The comfort gap widens with increasing costs of electricity p and narrows with better thermal

properties of the house β as well as a higher efficiency of the HVAC system γ_m. Furthermore, the comfort gap decreases with a higher comfort preference α.

Proposition 2.3 (Optimal Average Dispatch.) *The optimal average dispatch is linear in price and can be described by the following function,*

$$u^* = \begin{cases} \frac{1-\beta}{\gamma_m P_m \Delta t}|\theta^{com} - \theta^{out}| - \frac{(1-\beta)^2}{2\alpha\gamma_m^2 P_m \Delta t}p, & for \quad p < \frac{2\alpha\gamma_m}{1-\beta}\Delta\theta^{max}; \\ \frac{1-\beta}{m\gamma_m P_m \Delta t}(\theta^{com} + m\Delta\theta^{max} - \theta^{out}), & else. \end{cases} \quad (11)$$

Proposition 2.3 shows that optimal average dispatch increases if the cost of electricity decreases. It furthermore increases if the difference between the comfort and the outside temperature $|\theta^{com} - \theta^{out}|$ is higher (for instance during winter or summer) and the efficiency γ_m and rated power P_m of the HVAC system are lower. The effect of the thermal properties of the house β is ambivalent as better insulation requires less dispatch to maintain a certain temperature; on the other hand, dispatch is more valuable as the temperature improvement holds on for longer.

2.2.3 Implementation in a Smart Home System

We can implement the willingness-to-pay-based dispatch function as presented in Theorem 2.1 on the smart home system for automated bidding. To compute the willingness-to-pay b_t, the customer has to provide his comfort temperature θ^{com} and his comfort preference α. θ^{com} and α can be adjusted over time according to the customers' preferences, however, compared to the other parameters of the system, they are changing less often which is why we drop the time index for readability.

As customers are unlikely to have a specific understanding of their comfort preference α in numerical terms, the customer could provide it using a slider as displayed in Fig. 1a. Such a slider would represent the trade-off between comfort and costs and can be intuitively set by

the customer. Both parameters, the comfort preference α and the comfort temperature θ^{com}, can also be adjusted to changing circumstances, e.g. when the customer is not at home. In contrast, the parameters β and γ_m are physical characteristics of the system and customer behavior, but are not subject to customer choice.

Figure 1: Choice of comfort preference α
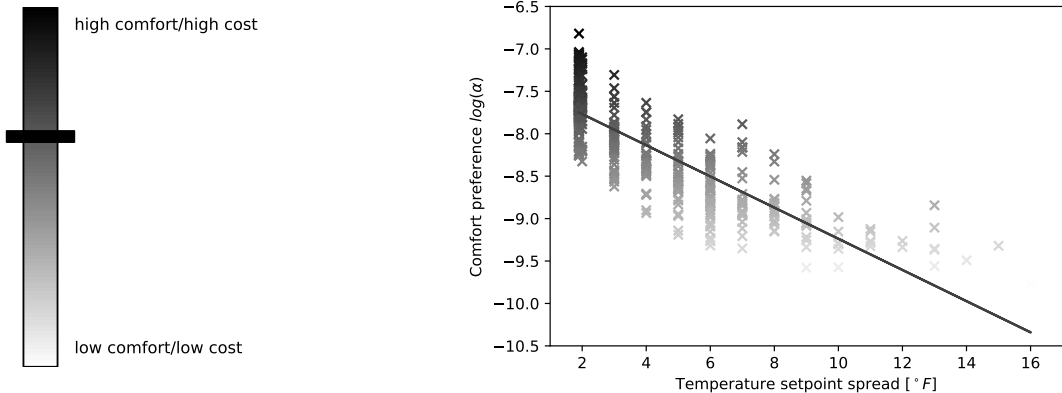
(a) Slider for comfort setting

(b) Translation of temperature setpoints into comfort preference (exemplary illustration for August 1 - 7, 2016)

Importantly, the design proposed by us does not require the customer to provide more information than under a fixed retail rate. While customers provide a heating and a cooling setpoint to conventional HVAC systems, in our system, the customer would provide the comfort preference α and the comfort temperature θ^{com}. Fig. 1b further shows how settings under a conventional system correspond to the settings under the system proposed by us: customers who provided a narrow temperature band for conventional HVAC operations are optimally entering a higher comfort preference α. Fig. 1b is an illustration of the parametrization of customers in our case study and we will describe the estimation of α as a function of temperature setpoints in more detail in Section 4.

During operations, at the beginning of each market interval t, the smart home system computes the real-time willingness-to-pay b_t and dispatches the HVAC system if the willingness-to-pay exceeds the energy price. In addition, the smart home system could submit the willingness-to-pay as a bid to participate in other economic coordination mechanisms

13

such as auctions. We describe the design of our proposal of such an auction-based local demand management system in the following Section 3.
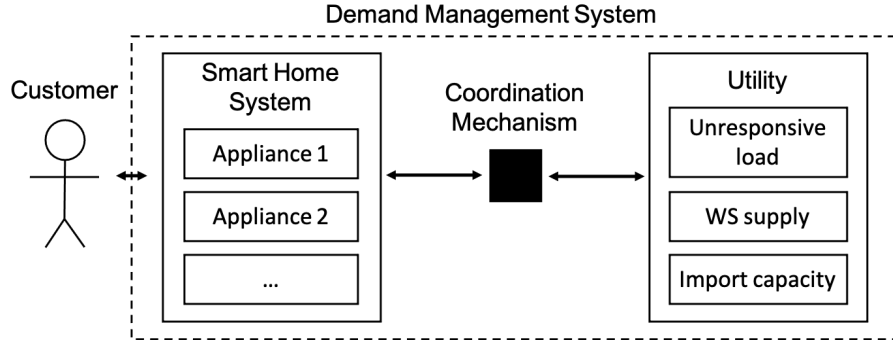
3 Management of Residential Distribution Systems

Figure 2: Components of demand management system

In the following, we describe how the automation of customer dispatch can be leveraged to efficiently manage electric distribution systems. Our demand management system is displayed by Fig. 2. On the demand side, all participating customers $i \in \mathcal{I}$ enter their preferences for the dispatch of flexible appliances through the smart home system (e.g. the preferred temperature for an HVAC system or the minimum range for an electric vehicle). At the beginning of each market interval t and separately for each appliance $j \in \mathcal{J}$, the smart home system combines these preferences with relevant physical information (e.g. the current temperature or state-of-charge of a battery) into the real-time willingness-to-pay b_t^j, using the approach described in Section 2. The willingness-to-pay b_t^j and the required power P^j over the duration Δt of the upcoming market interval are submitted to the operator of the demand management system as a demand bid. Unresponsive load of the customer, e.g. electric lighting, is not managed by the smart home system. Instead, the utility places a bid on behalf of the aggregate of unresponsive loads in the distribution system, based on an aggregate load forecast. Supply is imported by the utility and its cost c_t^{WS} can, for instance, correspond to the wholesale market price and a fixed mark-up for system-related costs, e.g.

14

grid losses or costs of operating the demand management system.

Once all demand bids have been submitted, the operator aggregates the demand function $D_t(p_t)$ (with $D'_t(p_t) \leq 0$) and evaluates demand at the real-time cost of electricity supply c_t^{WS}. The demand management system can take two states: unconstrained and constrained. If $D_t(p_t = c_t^{WS})$ is less or equal to the import constraint from the transmission system, all demand can be satisfied and the distribution system is unconstrained. Then, the clearing price p_t equals the supply cost from the wholesale market. If, however, $D_t(p = c_t^{WS})$ exceeds the import constraint, not all demand can be satisfied and the system is constrained. As a result, the clearing price p_t increases above the level of the supply costs c_t^{WS} until demand $D_t(p_t)$ is equal to or less than the import constraint. The market-clearing price p_t is then published and communicated to all automated appliances.

Based on the clearing price p_t, smart home systems can infer the dispatch of their appliances. An appliance j is dispatched if $b_t^j \geq p_t$ and is not dispatched if $b_t^j < p_t$. As customers have no advantage in misrepresenting their true willingness-to-pay when submitting b_t^j, this dispatch behavior is individually rational and the clearing result of the demand management system will indeed be implemented. Unresponsive loads are not sensitive to p_t and customers dispatch them as needed.

This system could, for instance, be operated by an integrated utility (investor-owned or member-owned). Utilities often incorporate the role of the monopolistic retailer and operator of the grid in residential distribution systems. Our system would provide them with the means to manage their systems more efficiently. Alternatively, it could be managed by a third party market operator.

Our demand management system represents a market-based coordination mechanism. It allows for the priority-based dispatch of flexible appliances, considering the real-time cost of supply. Market-based demand management system have been proposed by previous literature, see e.g. [3], [22], or [6]. We are, however, the first to propose a demand management system which integrates automated economic bidding through a smart home system with

15

real-time distribution system management. Future versions of our system could furthermore integrate local generation and storage or consider congestion within the distribution system.

4   Case Study

In this section, we present the setup of our case study, a residential distribution system with 437 customers. We detail the compilation of our distribution system model (Section 4.1), describe our simulation approach (Section 4.2), and present the calibration of the parameters of our model (Section 4.3). The purpose of the case study will be to evaluate the performance of our proposed bidding strategy and the demand management system on customer surplus and social welfare. The results will be presented in Section 5.

4.1   Data and Distribution System Model

We assemble a synthetic residential distribution system in Austin, Texas, with one connection point to the overlying grid. We use a standard IEEE electric feeder to represent the distribution grid [42] and populate it with 437 houses. This number is the result of a grid capacity analysis as described in Section 8. Specifically, we consider single-family homes and characterize the building stock based on [43] and [44]. This data provides information on the geography-specific floor area, house weatherization, HVAC system settings and parameters, etc. The base load of houses (non-flexible load) is derived from household data provided by [45] for the year 2016. HVAC systems are the dominant electric load and account for 75.5% of total residential electricity consumption in our system within a year. Previous work, e.g. [19], finds similar shares of HVAC loads in residential distribution systems. Finally, the distribution system is part of the Southern Load Zone in the Ercot system and imports electricity at real-time wholesale market prices. We use real-time prices for the year 2016 [46, 47]. More details on how our case study was assembled as well as a graphical illustration of the feeder are described in Section 8 in the appendix.

16

4.2 Simulation Approach

We use the distribution system simulation software GridLAB-D [48] to physically simulate residential customers and the electric distribution system. GridLAB-D includes simulation modules for a variety of residential load types, generation, and the electric grid. For our purpose, we use GridLAB-D's model of houses and HVAC systems. We create 437 house objects with randomly drawn physical characteristics according to the data described in Section 4.1. Importantly, GridLAB-D relies on a more complex thermal model to simulate internal temperature than the linear representation of the thermal model used by us in Section 2.2. However, this enables us to evaluate how our bidding strategy performs under realistic conditions despite the limited availability of future price and temperature information, as assumed in Section 2.2.3. All house objects are connected through the GridLAB-D representation of the electric grid and are served through a single import node. The distribution system is further exposed to changing local weather conditions provided by [49].

We run the simulation model in five minute intervals. Five minutes are a reasonable time interval during which HVAC systems can work efficiently. Under a fixed retail rate ('benchmark scenario'), HVAC systems dispatch according to the control provided by GridLAB-D. This control mimics conventional HVAC system control by keeping the internal temperature between the heating and the cooling setpoint. In particular, HVAC systems do not respond to price signals. We record the data on temperatures as well as household-level and distribution system-wide electric load to calibrate our utility model (see Section 4.3) and for the subsequent welfare analysis. Under our demand management system ('demand management system scenario'), at each time step, we use the values of the internal temperature provided by the simulation model and compute the willingness-to-pay of each household based on Section 2. Then, we run the market as described in Section 3 and determine the dispatch of the individual HVAC systems by comparing their willingness-to-pay to the resulting price. The latter replaces the conventional HVAC system control used in the benchmark scenario. At the end of each time step, we advance the simulation to the next time step and GridLAB-D

determines the new system parameters.

4.3 Calibration of Distribution System Model

To calibrate, we first simulate one year of operations under a fixed retail rate ('benchmark scenario'). Then, we leverage the temperature and dispatch time series to estimate house-specific parameters β and γ_m of Eq. (7), using linear regression. As building parameters as well as comfort preferences can change due to unobserved characteristics such as humidity or solar radiation, we estimate all parameters separately for each week of the year. Third, we determine the comfort preference α and the comfort temperature θ^{com} using the principle of revealed preferences, i.e. we calibrate the utility function of each customer such that the resulting optimal temperature setpoints correspond to the empirically given temperature setpoints under a fixed retail rate, as provided by [43]. The result of this estimation has been presented in Fig. 1b. Finally, we approximate P_m by the power which was needed when the appliance was last active in the given mode m. In contrast to the other parameters, we therefore update it on a regular basis as the power of the HVAC system can fluctuate due to grid and weather conditions. We do not assume that households constrain operations by minimum or maximum temperatures.

On the supply side, the supply cost c_t^{WS} corresponds to the wholesale market real-time price and a mark-up which accounts for grid losses. Grid losses are defined as the difference between the amount of electricity imported from the transmission grid and the electricity consumed by residential households. We calculate the mark up by computing the cost of grid losses in the benchmark scenario and dividing it by the total energy consumed by households.

Finally, all inelastic loads pay a fixed retail tariff. The cost of serving inelastic load corresponds to the difference between the total cost of import and the payments of flexible loads (including mark-ups). The fixed retail tariff is calculated in a budget-neutral way by dividing the cost of serving inelastic load by the amount of energy consumed by inelastic load. In the special case of no flexible load, i.e. the benchmark scenario under a fixed retail

rate, the cost of serving inelastic load corresponds to the total cost of import and is divided by the total amount of energy consumed. A separate billing of inelastic and elastic loads can be realized through the combination of the aggregate household meter and a sub-meter within the smart home system. Alternatively, all load could be metered according to the local real-time price through the aggregate household meter, with no impact on aggregate welfare effects of the demand management system.

5   Results

Using the case study introduced in Section 4, we first present the behavior of the system under a fixed retail rate ('benchmark scenario'; Section 5.1). Then, we quantify the implications of our demand management system on general welfare, residential customers, and the retailer in an unconstrained (Section 5.2) and a constrained system (Section 5.3).

5.1   Benchmark Scenario

In the benchmark scenario, customers face fixed retail rates and use a conventional, non-price-responsive HVAC control. Given this behavior, the average cost of a MWh imported to the distribution system is 27.01 USD/MWh and varies significantly throughout the year. Average procurement costs are minimal (13 to 15 USD/MWh) during the month of February and reach a maximum in the first week of August, with 68.91 USD/MWh. Maximum real-time prices can even reach a level of 1,772.80 USD/MWh, as on March 31, 2016. Furthermore, weeks exhibit very different levels of price variations, ranging from an unweighted standard deviation of 4.4 USD/MWh to a high level of 136.6 USD/MWh. This variability indicates potential savings under our demand management system from the system perspective. A detailed description can be found in Table 6 in the appendix.

The maximum of the system load is 2.311 MW. In 1% of the time, the load is equal or higher than 2.124 MW (91.9% of peak load) and, in 5% of the time, 1.723 MW (74.6%),

respectively. This indicates that high load levels only occur during a few hours or days within a year which determine the required import capacity. In general, high aggregate system load is driven by electricity consumption of HVAC systems during hot and cold temperatures in the middle of the summer (afternoons) and in the middle of the winter (mornings). Our demand management system could therefore contribute to flatten load and avoid expensive grid expansion. The complete load duration curve as well as weekly maximum load values can be found in the appendix, see Fig. 10 and Table 6.

5.2   Unconstrained System

In this section, we discuss the implications of our demand management system in an unconstrained system. The findings presented here also correspond to an alternative case where customers choose to individually implement the dispatch strategy described in Section 2.2.3 to respond to real-time prices, without a system-wide deployment of the demand management system as described in Section 3.

5.2.1   Welfare Effects

We calculate welfare changes as the change in aggregate customer comfort and energy procurement cost when switching from fixed retail tariffs to our demand management system. This perspective does not require any assumptions about the distribution of welfare gains between customers and the utility.

As a main result, we find substantial distribution system-wide welfare gains of automated HVAC system operations of up to 17,043 USD over the course of the year 2016. Fig. 3a shows realized welfare changes for the 51 full weeks of the year 2016 and their dependence on the standard deviation of the wholesale market price, weighted by system load. This figure allows for two important insights. First, we find that the system experiences significant welfare improvements in most weeks, reaching up to 1,918 USD within a week. There are two weeks for which the welfare change is slightly negative, adding up to a loss of 64 USD.

20

We attribute this finding to an imperfect description of the thermal dynamics of the system by the linear model and the myopic forecasting approach for external parameters. Second, the weighted standard deviation of the wholesale market price within a week is positively correlated with the achievable welfare change, by a coefficient of 0.85. With the standard deviation increasing by 1 USD/MWh, the prospective weekly welfare gain from switching from a fixed retail tariff to our demand management system increases by 11.00 USD.

Figure 3: Distribution of welfare changes
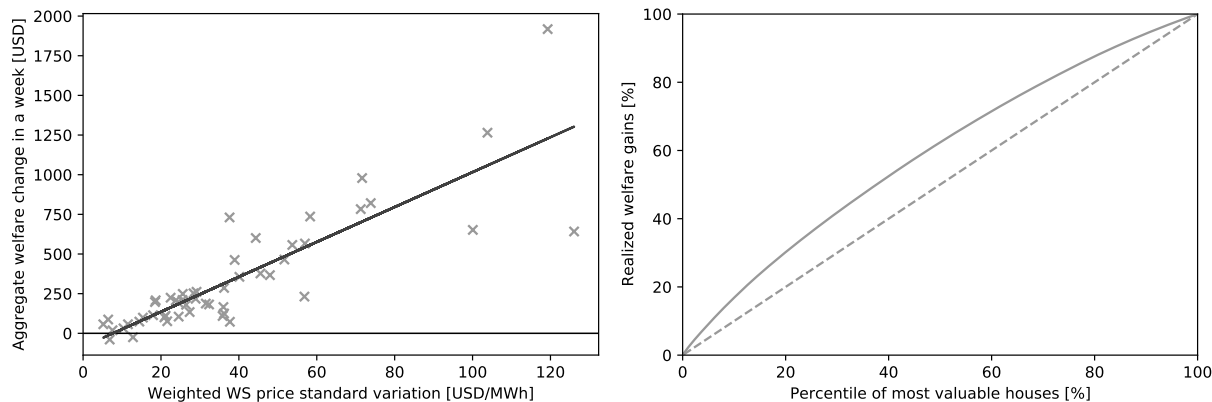
(a) Weekly welfare changes by weighted price standard deviation

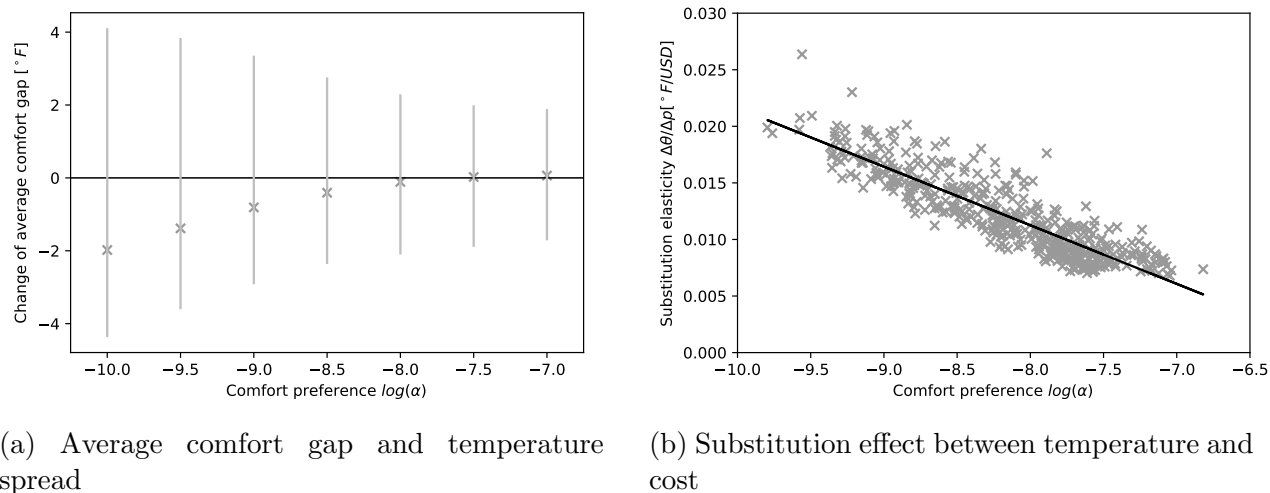(b) Cumulative welfare gain distribution over households

We moreover illustrate the distribution of welfare changes by households. Fig. 3b shows the cumulative distribution function of welfare changes, sorted from the house contributing the most to the one contributing the least to the overall welfare gain. The dashed line benchmarks our empirical finding with a hypothetical uniform distribution of welfare contributions. We find that all houses contribute positively to welfare . However, houses do not contribute equally to the welfare gain but, for instance, the 50% most valuable ones realize already 62.3% of possible welfare gains. The most valuable household contributes 92.86 USD while the least one contributes 18.53 USD.

5.2.2 Implications for Customers

The introduction of our demand management system impacts customers in two ways: through changes in comfort as well as their bills.

Comfort. Our evaluation framework allows to quantify the welfare changes associated with temperature variations induced by the demand management system. We find that the mean comfort change across households and throughout the year 2016 is -2.62 USD, with the maximum comfort increase of 17.88 USD and a maximum decrease of 26.75 USD. Customers with low comfort preference tend to experience comfort increases while those with high comfort preferences experience comfort losses. Fig. 12a and Fig. 12b provide more detailed evidence in the appendix.

Figure 4: Temperature as a function of comfort preference α (August 1 - 7, 2016)

(a) Average comfort gap and temperature spread

(b) Substitution effect between temperature and cost

We furthermore provide a detailed analysis of the internal temperature as the driver of comfort changes. As operating modes (i.e. heating/cooling) change between seasons, we focus on the first week of August (week 31). This week exhibits the highest average procurement costs (and, therefore, potential savings). It also requires frequent HVAC operations because of high outside temperatures. Under a fixed retail rate, customers' average comfort gap is $1.7°F$ (i.e. the absolute difference between the internal temperature and their comfort

temperature). The average comfort gap is larger than zero as the cost of electricity is positive (see Theorem 2.2). Under a demand management system, this gap reduces to $1.4°F$ or by 18.0%.

Fig. 4a details the dependence of the comfort gap change from the comfort preference of customers, aggregated by comfort preference classes of size $\Delta log(\widehat{\alpha}) = 0.5$ (e.g., $log(\widehat{\alpha}) = -8.0$ covers $log(\alpha) \in [-8.25, -7.75[$). We find that customers with the highest comfort preference hardly experience any changes of their comfort gap $(+0.1°F)$ while customers with the lowest comfort preference experience the largest improvement in the average comfort gap $(-2.0°F)$. As customers with low comfort preferences react particularly sensitively to price changes, they benefit from the time periods with real-time prices below the price level of the fixed retail rate. However, customers with low comfort preference also react particularly sensitively to high prices. As a consequence, customers with a low comfort preference α experience higher temperature variations. The bars of Fig. 4a represent the temperature spread which is defined as the difference of the 95% and the 5% quantiles of the temperature distribution. We find that, for customers with the lowest comfort preference, the temperature can oscillate up to $6.1°F$ above and $2.4°F$ below the comfort temperature. For customers with high comfort preference, this spread reduces to $+1.8°F$ and $-1.8°F$. In general, the temperature range under our demand management system is higher than under a fixed retail tariff and increases from $3.0°F$ to $4.8°F$, averaged over all customers.

Bill changes. We find that customers benefit from substantial bill savings. If the system is unconstrained, customers save 18,188 USD which corresponds to 41.62 USD per customer or 14.5%. These bill changes are driven by more cost-effective operations of HVAC systems which contribute 15,660 USD in savings. Moreover, the retail rate for unresponsive loads decreases compared to the benchmark scenario (given budget-neutrality as described in Section 4.3) and enables additional savings of 2,528 USD.

We furthermore provide an analysis of individual bill changes. In the benchmark scenario,

90% of the variance in bills for HVAC operations between customers are explained by the following parameters: bills increase with an increasing floor area (0.072 USD/sqf), decrease with improving thermal characteristics (-2,886.62 USD), and increase with increasing comfort preference (4.919e+05 $°F^2$). Furthermore, electricity bills are on average 44.09 USD less for houses which run on gas for heating. The summary of the regression results can be found in Table 7 in the appendix. Under our demand management system, absolute bill savings are highest for households with large electricity bills in the benchmark scenario (79% of variance). This indicates that consumers with a large impact on the system have a particularly high incentive to participate in our system (or switch to real-time prices). More details can be found in Table 8 in the appendix. The maximum total bill reduction per household is 140.36 USD, the minimum bill reduction 7.15 USD. The maximum relative bill saving per household is 21.4%, the minimum relative bill saving is 8.6%.
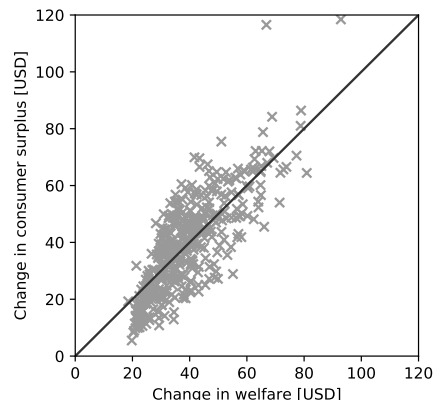
Total consumer surplus. Final consumer surplus is a combination of the changes in comfort and bills. Fig. 4b visualizes the empirical substitution effect between cost and comfort. Customers with a low comfort preference are willing to accept a temperature increase by up to 0.02 $°F$ if the electricity price increases by 1 USD/MWh. Customers with a high comfort preference only accept one fourth, on average. Fig. 5a shows the resulting distribution of house-specific consumer surplus changes. We find that consumer surplus increases consistently for all customers. The average surplus change is 39.00 USD, with a maximum of 118.46 USD and a minimum of 5.50 USD. Further details can be found in the appendix, see Fig. 13.

Finally, we investigate to which extent consumer surplus gains of houses coincide with their welfare contribution to the system, see Fig. 5b. We find that customers who contribute more to system welfare also experience higher consumer surplus gains. This means that the most valuable customers also have a strong private incentive to join the demand management system. However, we also observe that the most valuable customers experience an over-

Figure 5: Distribution of consumer surplus changes of houses
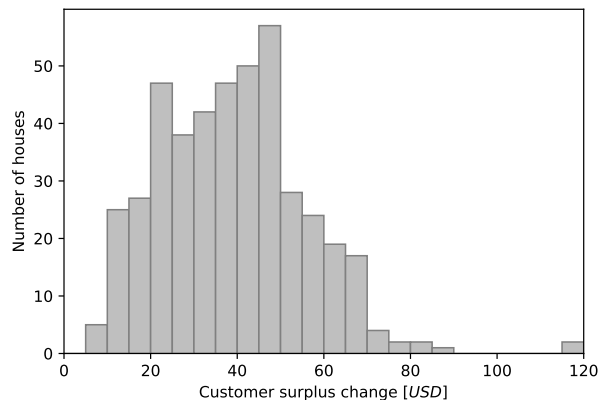
(a) Throughout the year

(b) Consumer surplus gains versus system welfare contribution

proportional gain in consumer surplus. Summarizing this and previous findings, consumer surplus gains are higher for customers with large floor sizes and such customers benefit over-proportionally compared to their individual contribution to welfare. This may indicate potential re-distribution effects between high- and low-income customers.

5.2.3   Implications for Utility

Table 2 summarizes the most important implications of our demand management system for the utility in an unconstrained system. We find that the amount of electricity imported by the utility increases slightly (by 2.4%). However, thanks to the fact that 75.4% of the consumption is price-responsive, energy procurement costs can be decreased by 14.6%. Compared to its share of 75.44% in consumption, the flexible load requires only an under-proportional share of procurement costs of 70.7%. Unresponsive loads benefit through a fixed retail rate which decreases by 75.5%, from 2.71 ct/kWh to 0.65 ct/kWh.

Eventually, we find that the peak load increases substantially by 26.7% to 2.5 MW, caused by the synchronization of HVAC systems by the price. Low prices and especially sudden price drops can lead to a synchronized dispatch of many HVAC systems. While this is individually rational and decreases the cost of energy procurement for the distribution

	No DMS	DMS
Energy procured [MWh]	4,608	4,717
Share of flexible load [%]	0.00	75.44
Procurement cost [USD]	125,063	106,851
Share of flexible procurement cost [%]	0.00	70.66
Average procurement price [USD/MWh]	27.14	22.66
Fixed retail rate [USD/kWh]	0.027	0.007
Total peak load [MW]	2.311	2.928

Table 2: Key measures of retail business with and without demand management system (DMS)

system, sudden load increases can be problematic from a system operations perspective [50]. In that case, the operator may clear the system subject to a temporary operational capacity constraint, as described in Section 5.3.

5.3 Constrained System

We further analyze the benefits of a demand management system in a constrained system. Fig. 6a demonstrates the ability of the system to integrate a capacity constraint for the peak day of the year, December 19, 2016. Under a fixed retail rate, the aggregated system load (solid light grey line) reaches the peak of 2.311 MW in the early morning hours, driven by electric heating. With the help of a demand management system, however, aggregate system load (dark grey solid line) can successfully be controlled around an exemplary capacity limit of 1.8 MW (dotted line). This is achieved by an increase in the local price. When there is no congestion, the local price equals the wholesale market price plus the mark-up for losses (1.69 USD/MWh). However, if the import constraint binds, the local price (dashed dark grey line) deviates from the real-time price of the wholesale market (dashed light grey line) by up to 20.76 USD/MWh. Local demand is reduced at the higher equilibrium price to equal import-constrained supply, especially during the morning hours until approximately 11am.

Fig. 6b further demonstrates how the load duration curve changes under different capacity constraints. Without our demand management system, the maximum load equals the year-

Figure 6: Implications of demand management system (DMS) for constraint management in distribution system (December 19 - 25, 2016)
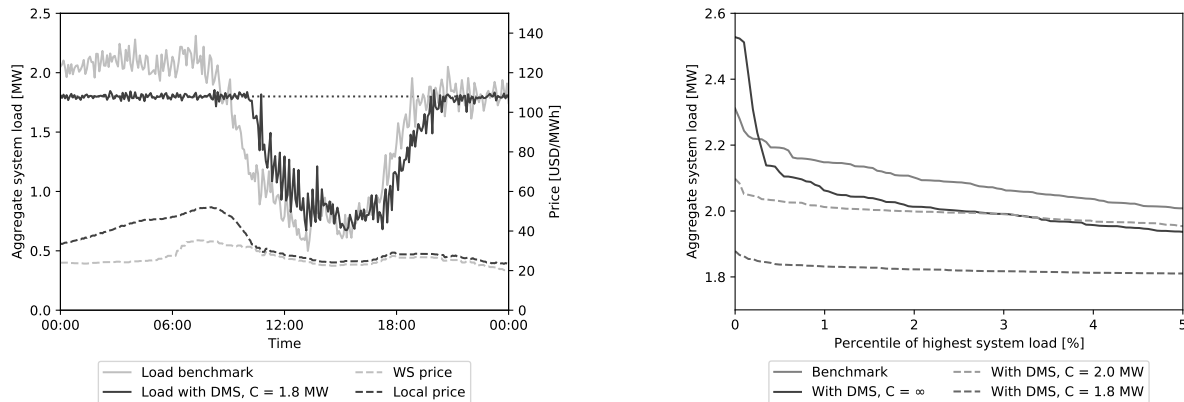

(a) Unmanaged and managed aggregated load on peak day (12/19/2016)

(b) Load curves under different scenarios for 5% quantile

long maximum of 2.3 MW. If a binding capacity constraint is imposed, aggregate load can generally be effectively controlled and decreased (here displayed for system constraints of 2.0 MW and 1.8 MW). It is notable that the aggregate system load can be nearly but not entirely reduced below the capacity constraint. There are multiple reasons for that. First, the system operator makes forecasting errors with regard to the unresponsive load. If the unresponsive load is under-estimated, too much capacity will be allocated to the flexible load and the resulting aggregate system load will exceed the capacity constraint. The maximum forecasting error is 141 kW. Second, the bids submitted might not correspond to the actual consumption of households. For instance, the power drawn by appliances can deviate from their rated power, depending on the grid conditions and other characteristics of the environment such as the outdoor temperature or the voltage quality in the system. Across market intervals, the maximum aggregate deviation caused by HVAC systems not complying with their bids is 25 kW. The errors introduced by these two channels are detailed in the appendix, see Fig. 11a and Fig. 11b. Third, system load can be too high if unresponsive load alone exceeds the capacity constraint.

Violating capacity limits can come at considerable cost, e.g. through the degradation of grid components or because of the dispatch of expensive reserve capacity (e.g. diesel

27

Figure 7: Welfare effects in a constrained system, example of the peak week (December 19 - 25, 2016)
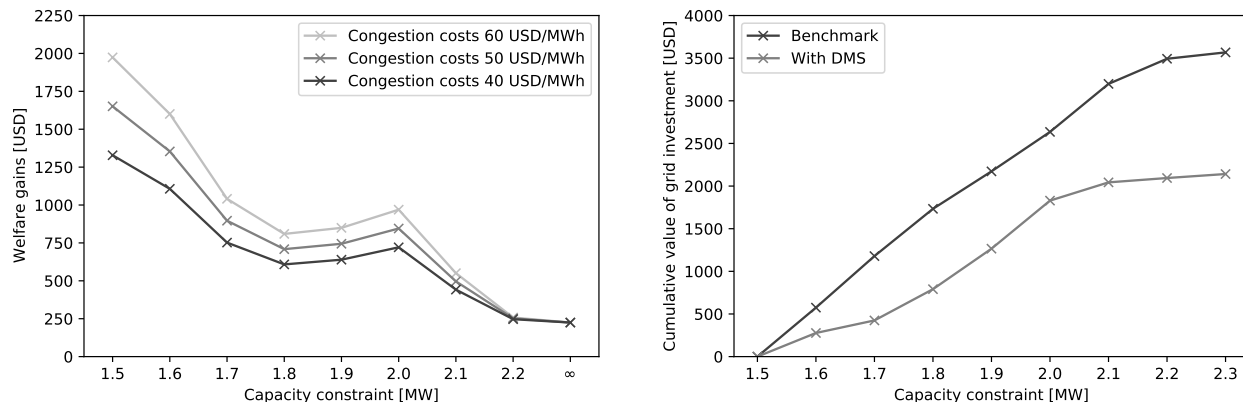
(a) Introducing a demand management system under a given constraint

(b) Expanding the grid, compared to a constraint of 1.5 MW

generators). We calculate these costs by multiplying the energy consumed by excess load with an estimate for per-unit congestion costs. In our analysis, we apply default cost of 50 USD/MWh which, for instance, corresponds to the marginal cost of operating a diesel generator. For the peak load week of December 19 - 25, 2016, congestion costs can add up to 3,568 USD if the system is constrained to 1.5 MW (the tightest system constraint included in this analysis). In that case, if our system is deployed, significant savings of 1,651 USD can be realized through its capability to manage load. Fig. 7a illustrates these savings for different capacity constraints and congestion costs. We find that the advantage of our demand management system over a fixed retail rate is generally higher for more constrained systems and higher per-unit congestion costs.

In practice, system operators and utilities also take advantage of other approaches to avoid load peaks, such as load shedding or energy efficiency measures. However, our demand management system has considerable advantages. First, while load shedding can likewise help to reduce or even avoid congestion costs, it is not able to realize welfare improvements during times without congestion nor does it allow for an efficient selection of loads to be shut down. For instance, during the system peak on December 19, 2016, at 7.15am, random load shedding would lead to a shut down of 34.5% of unresponsive load and keep HVAC

28

system with an average value of operations of 55.61 USD/MWh online. In contrast, our system would keep all unresponsive load as well as HVAC systems with an average value of operations of 61.52 USD/MWh online which corresponds to a welfare improvement. Second, energy efficiency measures could aim to reduce load by improving the insulation of houses and the efficiency of HVAC systems. While these measures can have an ambivalent effect on energy consumption (see Section 2.2.2), empirically, we find that better insulation and higher HVAC efficiency indeed decrease energy consumption under a fixed retail tariff, see Table 9. However, this is also the case under our demand management system. Therefore, energy efficiency measures and our system can rather be seen as complements.

According to [51], efficient investment in the grid infrastructure is the result of a trade off between short-term costs of congestion and long-term costs of grid investment. Fig. 7b provides an insight on the value of grid investment, using the peak load week of December 19 - 25, 2016 as an example. The value of grid investment is calculated as the difference between welfare under the new constraint (enabled by investment) and welfare under a constraint of 1.5 MW. We observe the following facts: first, relaxing import constraints increases welfare but less so if demand is managed. This indicates that, under demand management, less grid investment will be optimal than under a fixed retail rate, decreasing investment costs in the long-run. Considering the NPV estimate of 700 USD/kWh saved during the peak for delayed investment, as suggested by [9], savings could add up to to 357,700 USD (for a moderate reduction of the peak to 1.8 MW). Second, the marginal value of investment is not monotonously decreasing. In the benchmark scenario, it is highest between 2.0 and 2.1 MW and, with demand management, between 1.9 and 2.0 MW. This indicates that relaxing some levels of constraints can be particularly valuable and adds another layer of complexity to the optimal grid investment problem [e.g. 51, 52].

We finally investigate the market income of the operator of the demand management system. We define the market income as the income from importing at the wholesale market and re-selling at the local price. For that purpose, we analyze the market income for the

Capacity constraint [MW]	Market income [USD]
∞	0.00
2.2	3.03
2.1	4.35
2.0	8.92
1.9	96.20
1.8	362.29
1.7	848.95
1.6	1,439.96
1.5	2,084.60

Table 3: Market income under different capacity constraints for December 19 - 25, 2016

peak week of the year (December 19 - 25, 2016) under different constraints, as documented by Table 3. If no constraint applies, the market income from congestion is 0 USD as the local price corresponds to the cost of import. However, with the constraint of the grid being increasingly tight, the higher local price increases market income to more than 2,000 USD. This might create an incentive to withhold import capacity. As explained for Fig. 7b, the market income should ideally be invested in grid expansion. However, if the role of the operator of the demand management system is incorporated by the same entity which is responsible for grid enhancements, this might create an incentive to delay or under-size investment in the grid. Careful regulation can help to address a potential misalignment of incentives. In addition, regulation would need to consider the recovery of potential fixed cost associated with operating such a system.

6 Conclusion and Discussion

In this work, we proposed an integrated demand management system for load flexibility of customers in residential distribution systems with a potential constraint on maximum load. Our integrated demand management is characterized by an automated, real-time representation of customers' willingness-to-pay for dispatch by a smart home system and a market-based coordination of loads. Specifically, we suggested how the real-time willingness-

to-pay for Heating, Ventilation, and Air Conditioning (HVAC) systems can be conceptualized in a consistent economic framework and operationalized in a smart home system. We are convinced that this approach can also be used by other smart-grid related studies to improve the representation of demand and customer preferences. To evaluate the performance of our demand management system, we further deployed our approach in a case study of 437 houses with HVAC systems in Austin, Texas, and identified welfare gains of more than 17,000 USD. Moreover, we are the first to provide evidence of the distributional consequences of automation under real-time pricing for HVAC systems. We analyze welfare and consumer surplus changes for individual customers with different characteristics, provide insight into the redistribution of consumer surplus between customers when switching from fixed to real-time pricing, and establish how welfare changes with price volatility.

Our work has the following practical implications. First, previous work has demonstrated that automation plays a key role in accessing demand flexibility, especially when responding to quickly changing conditions [e.g. 27, 9]. We show that our real-time demand management system can realize substantial benefits by reducing demand in times of high prices or constrained import. Importantly, our dispatch strategy can also immediately be implemented in households independent from the demand management system and allow for automated response to a real-time price tariff. By doing so, customers could avoid peak price events and high bills such as during the recent Texas energy crisis [e.g. 33]. The increasing availability of smart home technologies [30, 31, 32, e.g.] can facilitate the implementation of real-time dispatch strategies, even for customers with low saving potential. Future work should experimentally validate our proposal and develop concepts for other services, e.g. electric vehicles, to advance our understanding of the interactions between human behavior, technology, and markets [53].

Second, [38] have further highlighted that the distributional consequences of time-dependent pricing can be substantial. We are the first to provide evidence on these effects under automation and for HVAC systems, an appliance owned by a large share of the population.

By doing so, we provide information for policy makers involved in the development and regulation of new tariffs. This concerns, for instance, the recent roll-out of time-of-use tariffs in California [54] or the prohibition of wholesale-market-based retail pricing in Texas [55]. Future work should advance the understanding on how automation affects different groups of customers and develop concepts which enable a fair distribution of the cost and benefits. We hope that an improved design of customer-friendly automation strategies and a better understanding of the potentials in residential distribution systems will facilitate a more efficient management of power systems, without compromising acceptance for dynamic incentives and enabling technologies.

Acknowledgements

References

[1] Y. Lin, P. Barooah, and J. L. Mathieu, "Ancillary services to the grid from commercial buildings through demand scheduling and control," *Proceedings of the American Control Conference (ACC 2015)*, pp. 3007–3012, 2015.

[2] E. Vrettos and G. Andersson, "Scheduling and Provision of Secondary Frequency Reserves by Aggregations of Commercial Buildings," *IEEE Transactions on Sustainable Energy*, vol. 7, no. 2, pp. 850–864, 2016.

[3] D. J. Hammerstrom, "Pacific Northwest GridWise(TM) Testbed Demonstration Projects Part I . Olympic Peninsula Project," tech. rep., 2007.

[4] S. Widergren, A. Somani, K. Subbarao, C. Marinovici, J. Fuller, J. Hammerstrom, and D. P. Chassin, "AEP Ohio gridSMART Demonstration Project Real-Time Pricing Demonstration Analysis," 2014. ed. PNNL.

[5] L. Ableitner, V. Tiefenbeck, A. Meeuw, A. Wörner, E. Fleisch, and F. Wortmann, "User behavior in a real-world peer-to-peer electricity market," *Applied Energy*, vol. 270, no. 2020, p. 115061, 2020.

[6] A. Wörner, L. Ableitner, A. Meeuw, F. Wortmann, and V. Tiefenbeck, "Peer-to-peer energy trading in the real world: Market design and evaluation of the user value proposition," *40th International Conference on Information Systems (ICIS)*, 2019.

[7] D. Adelman and C. Uçkun, "Crosscutting Areas—Dynamic Electricity Pricing to Smart Homes," *Operations Research*, vol. 67, no. 6, pp. 1520–1542, 2019.

[8] S. Borenstein, "The Long-Run Efficiency of Real Time Electricity Pricing," *The Energy Journal*, vol. 26, no. 3, pp. 93–116, 2005.

[9] B. K. Bollinger and W. R. Hartmann, "Information vs. Automation and implications for dynamic pricing," *Management Science*, vol. 66, no. 1, pp. 290–314, 2020.

[10] S. Borenstein and S. Holland, "On the Efficiency of Competitive Electricity Markets with Time-Invariant Retail Prices," *The RAND Journal of Economics*, vol. 36, no. 3, pp. 469–493, 2005.

[11] S. Borenstein, "Customer risk from real-time retail electricity pricing: Bill volatility and hedgability," *Energy Journal*, vol. 28, no. 2, pp. 111–130, 2007.

[12] N. Chen and G. Gallego, "Welfare analysis of dynamic pricing," *Management Science*, vol. 65, no. 1, pp. 139–151, 2019.

[13] A. G. Kök, K. Shang, and S. Yücelc, "Impact of electricity pricing policies on renewable energy investments and carbon emissions," *Management Science*, vol. 64, no. 1, pp. 131–148, 2018.

[14] S. Comello and S. Reichelstein, "The emergence of cost effective battery storage," *Nature Communications*, vol. 10, no. 1, pp. 1–9, 2019.

[15] Kök, A. Gürhan, Shang, Kevin, and Yücel, Safak, "Investments in Renewable and Conventional Energy: The Role of Operational Flexibility," *Manufacturing & Service Operations Management*, vol. 22, no. 5, 2020.

[16] S. P. Singh and A. Scheller-Wolf, "That's Not Fair: Tariff Structures for Electric Utilities with Rooftop Solar," *Manufacturing & Service Operations Management (ahead of print)*, Jan. 2021.

[17] H. Allcott, "Rethinking real-time electricity pricing," *Resource and Energy Economics*, vol. 33, no. 4, pp. 820–842, 2011.

[18] F. A. Wolak, "Do residential customers respond to hourly prices? Evidence from a dynamic pricing experiment," *American Economic Review*, vol. 101, no. 3, pp. 83–87, 2011.

[19] J. Burkhardt, K. Gillingham, and P. K. Kopalle, "Experimental Evidence on the Effect of Information and Pricing on Residential Electricity Consumption," *NBER Working Paper Series*, no. 25576, 2019.

[20] K. Valogianni, W. Ketter, J. Collins, and D. Zhdanov, "Sustainable Electric Vehicle Charging using Adaptive Pricing," *Production and Operations Management*, vol. 29, no. 6, pp. 1550–1572, 2020.

[21] J. K. Kok, C. J. Warmer, and I. G. Kamphuis, "PowerMatcher: Multiagent Control in

the Electricity Infrastructure," in *Proceedings of the 4th International Joint Conference on Autonomous Agents and Multiagent Systems (AAMAS 2005)*, p. 75, 2005.

[22] E. Mengelkamp, J. Gärttner, and C. Weinhardt, "Decentralizing energy systems through local energy markets: The LAMP-project," *Proceedings of the 2018 Multikonferenz Wirtschaftsinformatik (2018 MKWI)*, pp. 924–930, 2018.

[23] Z. Liu, Q. Wu, S. S. Oren, S. Huang, R. Li, and L. Cheng, "Distribution Locational Marginal Pricing for Optimal Electric Vehicle Charging Through Chance Constrained Mixed-Integer Programming," *IEEE Transactions on Smart Grid*, vol. 9, pp. 644–654, Mar. 2018.

[24] A. Rassa, C. van Leeuwen, R. Spaans, and K. Kok, "Developing Local Energy Markets: A Holistic System Approach," *IEEE Power and Energy Magazine*, vol. 17, pp. 59–70, Sept. 2019.

[25] A. Dimeas and N. Hatziargyriou, "Operation of a multiagent system for microgrid control," *IEEE Transactions on Power Systems*, vol. 20, pp. 1447 – 1455, 09 2005.

[26] A. Radovanovic, A. Ramesh, R. Koningstein, D. Fork, W. Weber, S. Kim, J. Schmalzried, J. Sastry, M. Dikovsky, K. Bozhkov, E. Pinheiro, C. Lebsack, S. Collyer, A. Somani, R. Rajagopal, A. Majumdar, J. Qin, G. Cezar, J. Rivas, A. El Gamal, D. Gruenich, S. Chu, and S. Kiliccote, "Powernet for distributed energy resource networks," *IEEE Power and Energy Society General Meeting 2016*, 2016.

[27] A. Faruqui and S. Sergici, "Household response to dynamic pricing of electricity: A survey of 15 experiments," *Journal of Regulatory Economics*, vol. 38, no. 2, pp. 193–225, 2010.

[28] K. Seddig, P. Jochem, and W. Fichtner, "Two-stage stochastic optimization for cost-minimal charging of electric vehicles at public charging stations with photovoltaics," *Applied Energy*, vol. 242, no. 2019, pp. 769–781, 2019.

[29] G. Graber, V. Calderaro, P. Mancarella, and V. Galdi, "Two-stage stochastic sizing and packetized energy scheduling of BEV charging stations with quality of service con-

straints," *Applied Energy*, vol. 260, no. 2020, p. 114262, 2020.

[30] Facts & Factors, "Smart Home Systems Market By Technology (Cellular Network Technologies, Protocols & Standards, Wireless Communication Technologies), By Product (Lighting Control, Security & Access Control, HVAC Control, Media & Entertainment & Others), And By Regions - Global & Regional Industry Perspective, Comprehensive Analysis, and Forecast 2021 – 2026," tech. rep., 2021.

[31] Mordor Intelligence, "North America Smart Homes Market - Growth, Trends, COVID-19 Impact, and Forecasts (2022 - 2027)," tech. rep., 2021.

[32] MarketsandMarkets, "Smart Home Market with COVID-19 Impact Analysis by Product (Lighting Control, Security & Access Control, HVAC Control, Smart Speaker, Smart Kitchen, Smart Furniture), Software & Services, Sales Channel, and Region – Global Forecast to 2026," tech. rep., 2021.

[33] G. McDonnell Nieto del Rio, N. Bogel-Burroughs, and I. Penn, "His Lights Stayed on During Texas' Storm. Now He Owes $16,752 (published on Feb 20, 2021)," *New York Times*, 2021.

[34] CAISO, "Transmission Economic Assessment Methodology (TEAM)," tech. rep., 2017.

[35] ENTSO-E, "ENTSO-E Guideline for Cost Benefit Analysis of Grid Development Projects," tech. rep., 2018.

[36] CAISO, "Resource Adequacy," 2020. https://www.cpuc.ca.gov/ra/, last access on 2020-07-04.

[37] PJM, "PJM Capacity Market & Demand Response Operations," 2020. PJM Manual 18, Revision 45, effective as of 2020-05-28.

[38] S. Burger, C. R. Knittel, I. J. Pérez-Arriaga, I. Schneider, and F. vom Scheidt, "The Efficiency and Distributional Effects of Alternative Residential Electricity Rate Designs," *NBER Working Paper Series*, no. 25570, 2019.

[39] P. Baake, S. Schwenen, and C. von Hirschhausen, "Local Power Markets," *SSRN Electronic Journal*, 2020.

[40] P. Fanger, *Thermal comfort. Analysis and applications in environmental engineering.* Copenhagen: Danish Technical Press, 1970.

[41] J. L. Mathieu, S. Koch, and D. S. Callaway, "State estimation and control of electric loads to manage real-time energy imbalance," *IEEE Transactions on Power Systems*, vol. 28, no. 1, pp. 430–440, 2013.

[42] IEEE Power Engineering Society, "IEEE 123 Node Test Feeder," 2014. `https://site.ieee.org/pes-testfeeders/resources/`, last access on 2020-07-04.

[43] US Energy Information Administration, "Residential Energy Consumption Survey (RECS)," 2015. `https://www.eia.gov/consumption/residential`, last access on 2020-04-18.

[44] US Environmental Protection Agency, "Energy Star: Home Sealing Specification," tech. rep., 2001.

[45] Inc. Pecan Street, "Pecan Street," 2019.

[46] Ercot, "Market Prices," 2019. `http://www.ercot.com/mktinfo/prices`, last access on 2019-11-25.

[47] Ercot, "Settlement Points List and Electrical Buses Mapping," 2020. `http://mis.ercot.com/misapp/GetReports.do?reportTypeId=10008&reportTitle=Settlement%20Points%20List%20and%20Electrical%20Buses%20Mapping&showHTMLView=&mimicKey`, last access on 2021-03-01.

[48] SLAC, "GridLAB-D 4.2.0-191209 (master) Linux (2019)," 2019.

[49] NREL, "National Solar Radiation Data Base," 2015. `https://rredc.nrel.gov/solar/old{_}data/nsrdb/1991-2005/tmy3/by{_}state{_}and{_}city.html`, last access on 2019-12-06.

[50] Y. Parag and B. K. Sovacool, "Electricity market design for the prosumer era," *Nature Energy*, vol. 1, no. 4, 2016.

[51] P. Joskow and J. Tirole, "Merchant Transmission Investment," *The Journal of Industrial Economics*, vol. 53, no. 2, pp. 233–264, 2005.

[52] T. Lohmann and S. Rebennack, "Tailored benders decomposition for a long-term power expansion model with short-term demand response," *Management Science*, vol. 63, no. 6, pp. 2027–2048, 2017.

[53] Y. Chen, P. Cramton, J. A. List, and A. Ockenfels, "Market Design, Human Behavior, and Management," *Management Science*, no. Articles in Advance, 2020.

[54] PGE, "Transition to Time-of-Use," 2021. `https://www.pge.com/en_US/residential/rate-plans/rate-plan-options/time-of-use-base-plan/time-of-use-plan/time-of-use-transition.page?`, last access on 2021-08-24.

[55] Texas, "HB 16. Relating to the regulation of certain retail electric products," 2021. Effective on 2021-09-01.

[56] Ercot, "ERCOT Monthly Operational Overview: September," tech. rep., 2018.

7 Derivation of HVAC Willingness-to-Pay Function

On average, the optimal internal temperature stays constant if prices and outside temperature stay constant under the myopicity assumption, i.e. $\theta_t = \theta_{t+1} = \theta$. Therefore, we can re-write the transition function Eq. (7) for the average internal temperature as follows,

$$\theta = \beta\theta + (1 - \beta)\theta^{out} + m\gamma_m P_m \Delta t u. \tag{12}$$

Re-arranging Eq. (12) allows to describe the relationship between the average temperature θ and the average dispatch u,

$$u(\theta) = \frac{1 - \beta}{m\gamma_m P_m \Delta t}(\theta - \theta^{out}). \tag{13}$$

We insert Eq. (13) into the objective function Eq. (14),

$$\max_u [-\alpha(\Delta\theta)^2 - p\frac{1 - \beta}{m\gamma_m}(\theta - \theta^{out}))] \tag{14}$$

To solve for an inner solution, we take the first derivative with respect to θ and subsequently solve for p which corresponds to the willingness-to-pay b for a comfort level θ,

$$\frac{d}{d\theta}[-\alpha(\Delta\theta)^2 - p\frac{1 - \beta}{m\gamma_m}(\theta - \theta^{out}))] = -2\alpha\Delta\theta - p\frac{1 - \beta}{m\gamma_m} \overset{!}{=} 0 \tag{15}$$

Re-arranging gives Theorem 2.1. Alternatively, solving Eq. (14) for the optimal average dispatch u^* leads to Theorem 2.3. Inserting into Eq. (13) further allows to derive the optimal temperature level θ^*, as described in Proposition 2.2.

For extreme temperatures, the constraints with regard to θ^{min} and θ^{max} become binding. The respective solutions follow directly from applying the maximum average comfort gap $\Delta\theta_m^{max}$. The latter is defined as the difference between the maximum ($m = -1$) or minimum ($m = 1$) average temperature of a cycle and the comfort temperature. The maximum average

temperature of a cycle is the average temperature of a cycle where $\theta^{least} = \theta^{max}$,

$$\frac{\theta^{max} + \theta^{most}}{2} = \frac{\theta^{max} + (\beta\theta^{max} + (1-\beta)\theta^{out} - \gamma_c P_c \Delta t)}{2}$$

$$= \frac{(1+\beta)\theta^{max} + (1-\beta)\theta^{out} - \gamma_c P_c \Delta t}{2} \quad (16)$$

Accordingly, the maximum average comfort gap $\Delta\theta_c^{max}$ for cooling is defined as follows,

$$\Delta\theta_c^{max} = \frac{(1+\beta)\theta^{max} + (1-\beta)\theta^{out} - \gamma_c P_c \Delta t}{2} - \theta^{com}. \quad (17)$$

Equivalently, the maximum average comfort gap $\Delta\theta_h^{max}$ for heating is defined as follows,

$$\Delta\theta_h^{max} = |\frac{(1+\beta)\theta^{min} + (1-\beta)\theta^{out} + \gamma_h P_h \Delta t}{2} - \theta^{com}|. \quad (18)$$

For Eq. (11), we directly insert the constraints θ^{min} and θ^{max} into Eq. (13), respectively, with $\theta^{min} = \theta^{com} - \Delta\theta_h^{max}$ and $\theta^{max} = \theta^{com} + \Delta\theta_c^{max}$.

8 Data and Feeder Assembly

House data. We generate houses based on survey data provided by [43]. For each house, we randomly draw the number of stories (one or two) and the floor area according to the mean and standard deviation provided. With regard to the thermal system, we consider the most important technologies: resistive heating, heat pump, and natural gas (for heating) as well as electric cooling with or without a heat pump (for cooling). For each feasible combination, the probabilities for a house operating a certain type of HVAC system as well as heating and cooling setpoints are estimated based on the data for the West South Central CENSUS region provided by the [43]. For the other technical characteristics, we use the recommendations for default parameters as provided by GridLAB-D [48]. Table 4 and Table 5 summarize the parameters. Furthermore, we calculate natural air changes by hour for one and two story buildings in Zone 2 under normal conditions, using the ACH_{50} value specific to climate zone 2A and the LBL factor provided by [44]. Residential base load follows smart meter data published by the Pecan Street data project [45]. We use a subset containing all data from Austin for the year 2016 because the number of distinct base load profiles is highest (108).

Feeder. We model the physical network using the IEEE 123 feeder which represents a typical residential distribution grid. The feeder has a single connection to the overlying grid. The feeder branches out into multiple sub-feeders, representing streets. A graphical illustration of the feeder is displayed by Fig. 8.

We further established a routine to populate the feeder to build an electrically balanced distribution system. We accommodate 2,000 detached single-family houses for an initial hosting capacity analysis. Houses are randomly generated according to the data provided at the beginning of this section. We simulate electric load for the month of July, using GridLAB-D [48]. We determine the average power per house at the time of maximum load, the After Diversity Maximum Demand (ADMD) factor, which is 4.59 kW. In a second step,

Parameter	Average Value	Standard Deviation	Share [%]
Floor size $[ft^2]$			
- 1 story	1976.96	47.05	72.09
- 2 stories	3202.38	226.41	27.91
Heating [%]			
- resistive			49.60
- heat pump			8.80
- natural gas			41.60
Cooling [%]			
- heat pump			83.04
- electric, no heat pump			16.07
Setpoints $[°F]$			
- heating	70.77	2.93	
- cooling	73.70	3.33	

Table 4: Parametrization of detached single-family houses (West South Central) [43]

HVAC System	1 story	2 stories
Electric cooling / NG heating	24.90%	9.64%
Electric cooling / resistive heating	29.69%	11.49%
Heat pump	17.50%	6.77%

Table 5: HVAC system statistics for housing types [43]

we use this factor to randomly assign houses to nodes of the IEEE123 feeder while respecting the maximum hosting capacity of each node. The latter is provided by the specifications of the IEEE123 model [42]. We determine the design capacity by multiplying this value with a safety factor of 0.66 and iteratively assign houses to nodes until none of the nodes is able to accommodate more load of the size described by the ADMD anymore. We find that 437 houses in total can be accommodated. The maximum hosting capacity is 3.6 MW.

Price data. We use Ercot price data. Austin is part of the Southern Hub [56] and we use the historical price data for 2016 which is available for the Southern Hub in 15 minute intervals for the Real-Time market [46].
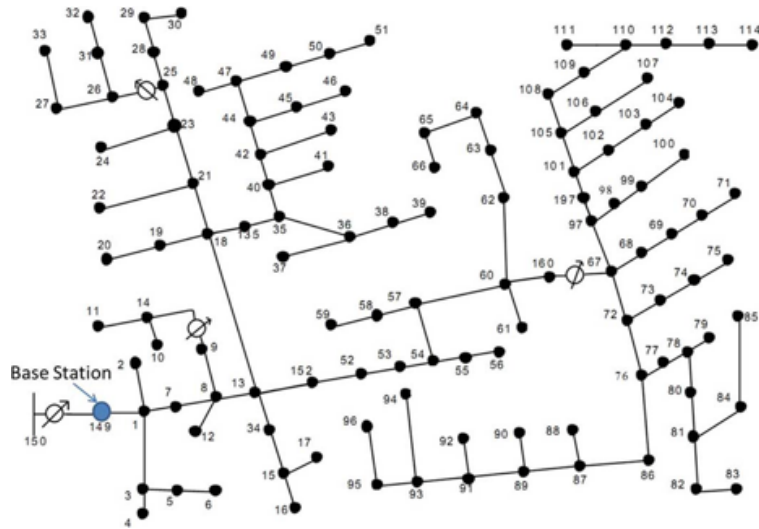
Figure 8: IEEE 123 feeder [42]

Weather data. We use tmy3 data (722540TYA) for Austin [49] which represents hourly local median weather conditions, including temperature, solar radiation, and wind speed.

9 Detailed Results for Base Case

Week	Av. procurement cost [USD/MWh]	Max. price [USD/MWh]	Standard deviation price [USD/MWh]	Max. load [MW]
01/04 - 01/10	20.76	639.13	26.023	2.116
01/11 - 01/17	17.03	355.41	24.656	1.539
01/18 - 01/24	17.73	340.31	14.373	2.260
01/25 - 01/31	21.87	306.75	42.504	1.802
02/01 - 02/07	13.45	61.67	4.387	1.818
02/08 - 02/14	14.71	108.95	6.675	1.453
02/15 - 02/21	14.53	363.37	26.223	1.441
02/22 - 02/28	14.65	972.00	45.911	1.462
02/29 - 03/06	14.70	360.59	28.310	1.316
03/07 - 03/13	23.25	538.92	50.576	1.731
03/14 - 03/20	33.40	277.84	38.529	1.281
03/21 - 03/27	20.43	799.56	44.566	0.995
03/28 - 04/03	26.73	1772.80	136.637	1.430
04/04 - 04/10	17.47	350.21	20.482	1.241
04/11 - 04/17	19.48	211.40	16.814	1.484
04/18 - 04/24	32.33	235.26	28.651	1.369
04/25 - 05/01	32.79	1507.76	72.479	1.348
05/02 - 05/08	18.95	500.21	28.521	1.244
05/09 - 05/15	29.81	638.87	34.401	1.346
05/16 - 05/22	30.88	860.73	61.269	1.615
05/23 - 05/29	27.30	415.24	29.861	1.471
05/30 - 06/05	21.23	165.89	9.796	1.454
06/06 - 06/12	26.83	338.21	20.587	1.714
06/13 - 06/19	27.97	214.30	13.541	1.599
06/20 - 06/26	25.14	163.41	8.543	1.622
06/27 - 07/03	33.72	548.80	28.132	1.523
07/04 - 07/10	26.97	183.80	12.440	1.684
07/11 - 07/17	28.81	397.44	21.364	1.652
07/18 - 07/24	46.52	665.79	50.329	2.079
07/25 - 07/31	34.72	693.30	38.253	1.659
08/01 - 08/07	68.91	899.52	86.736	1.674
08/08 - 08/14	34.30	221.10	15.130	1.621
08/15 - 08/21	25.08	313.94	18.239	1.751
08/22 - 08/28	34.16	377.76	30.518	1.698
08/29 - 09/04	26.34	64.64	5.753	1.536
09/05 - 09/11	29.20	297.98	20.420	1.514
09/12 - 09/18	55.08	871.30	71.342	1.383
09/19 - 09/25	35.22	417.36	26.327	1.231
09/26 - 10/02	31.32	319.19	21.474	1.421

Week	Av. procurement cost [USD/MWh]	Max. price [USD/MWh]	Standard deviation price [USD/MWh]	Max. load [MW]
10/03 - 10/09	48.31	734.63	46.305	1.448
10/10 - 10/16	27.75	329.99	14.999	1.316
10/17 - 10/23	24.96	749.98	35.899	0.985
10/24 - 10/30	28.77	443.80	24.266	1.123
10/31 - 11/06	23.81	379.71	17.515	1.257
11/07 - 11/13	17.50	271.73	11.926	1.246
11/14 - 11/20	18.87	450.85	22.181	0.958
11/21 - 11/27	20.70	340.64	24.628	1.176
11/28 - 12/04	28.19	812.22	72.477	1.654
12/05 - 12/11	24.75	504.45	30.528	1.501
12/12 - 12/18	20.78	505.19	23.617	2.194
12/19 - 12/25	21.22	398.08	24.170	2.311

Table 6: Load and price summary for each week of the year 2016

Table 6 presents key figures for each week of the simulation year 2016. The first three columns provide information on the energy procurement cost. The average procurement cost describes the weighted average price which the retailer pays for each unit of energy [MWh] imported from the wholesale market. The maximum price corresponds to the maximum real-time price on the wholesale market during this week. The standard deviation of the wholesale market price reflects the price variability during the week. The last column provides the maximum feeder load, measured at the connection point to the aggregate system level. The feeder load is important for the sizing of the transformer at the connection to the aggregate system level and a relevant cost driver.

Fig. 9 shows the resulting average system load for each hour of the day in each month of the year, as measured at the point of connection to the aggregate system level. Summer months are depicted in dark colours, winter months in light colours. We use dashed lines to represent the months of the first half of the year and solid lines for the months of the second half.

Fig. 10 shows the load duration curve of the system for the whole year, i.e. for what share of the time a certain load level or higher is reached.
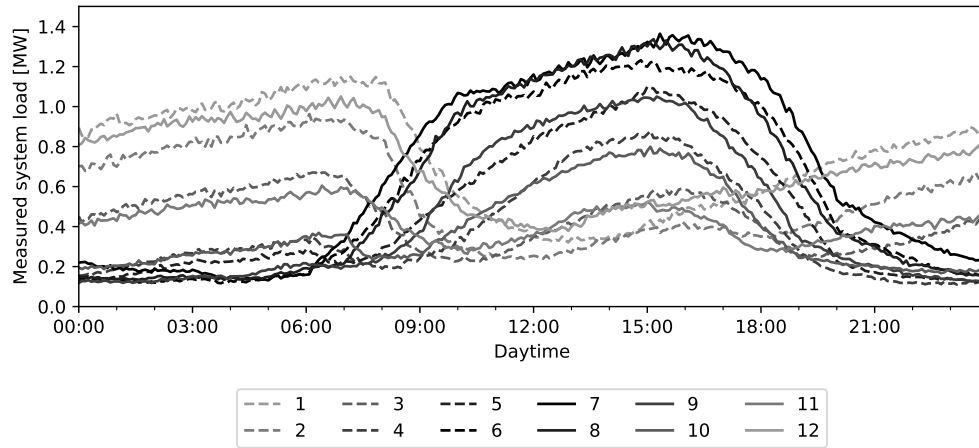
Figure 9: Average hourly aggregate system load for each month, from January ('1') to December ('12')
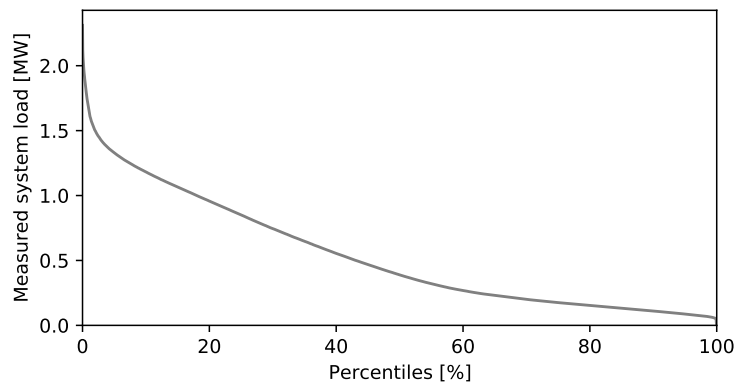

Figure 10: Load duration curve over the year 2016

47

	Dependent variable:
	Electricity bill
const	2762.033***
	(148.145)
floor area	0.072***
	(0.002)
α	491943.471***
	(22039.625)
β	-2886.618***
	(157.644)
has gas heating	-44.094***
	(3.372)
Observations	437
R^2	0.903
Adjusted R^2	0.902
Residual Std. Error	25.647(df = 432)
F Statistic	1002.101*** (df = 4.0; 432.0)
Note:	*p<0.1; **p<0.05; ***p<0.01

Table 7: OLS regression results: Determinants of electricity bills under a fixed retail rate

Table 7 illustrates to which extent house-specific parameters explain the electricity bills under a fixed retail rate (benchmark scenario). We find that bills are driven by the floor area, comfort preference, thermal characteristics, and gas versus electricity-based heating.

10 Detailed Results for Case Study

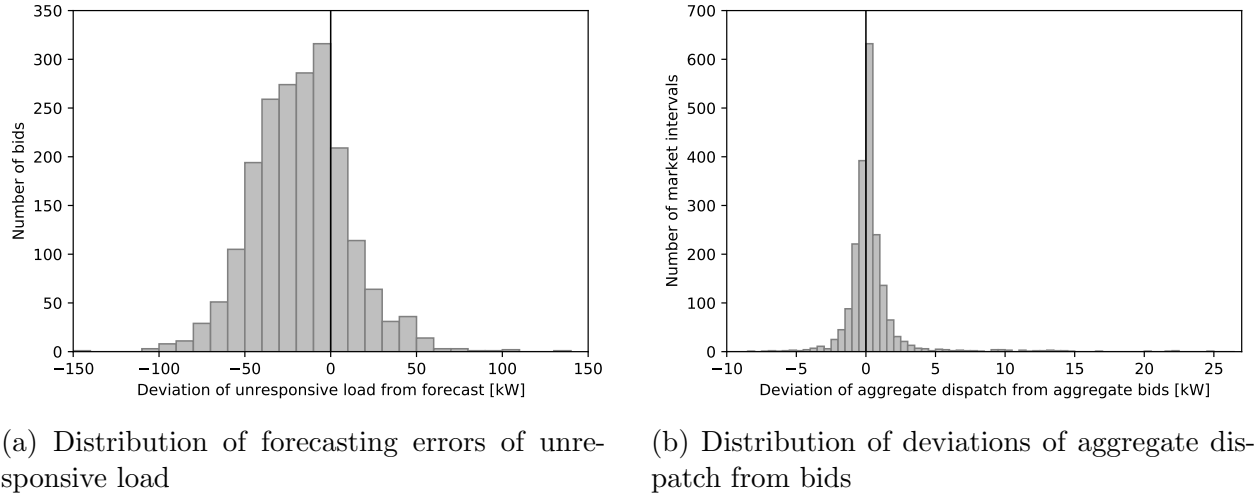Figure 11: Deviations of physical dispatch from market result (December 19-25, 2016)

(a) Distribution of forecasting errors of unresponsive load

(b) Distribution of deviations of aggregate dispatch from bids

Fig. 11a illustrates the retailer's forecasting errors with regard to the unresponsive load. The unresponsive load covers the base load of customers as well as grid losses. Fig. 11a shows that the actual unresponsive load tends to be over-estimated. The maximum absolute deviation is 141 kW. Furthermore, system imbalances can occur if the actual dispatch of flexible appliances deviate from the bid submitted to the operator of the demand management system. Fig. 11b shows the distribution of such deviations, aggregated over all customers within a market interval. While deviations exist, they are distributed close to zero, with a maximum net deviation of 25 kW. This is much less than the error introduced by the unresponsive load forecast and suggests that potential deviations are not or only slightly correlated across devices.

Fig. 12a displays the distribution of consumer surplus changes attributed to internal temperature changes, i.e. comfort changes. This is detailed by Fig. 12b which additionally shows the comfort change as a function of the comfort preference α. While households with a low comfort preference largely experience positive comfort changes, we observe a deterioration in comfort for households with high comfort preferences. Despite only small temperature changes as indicated by Fig. 4a, such households evaluate these deviations

Figure 12: Consumer surplus changes attributed to comfort change
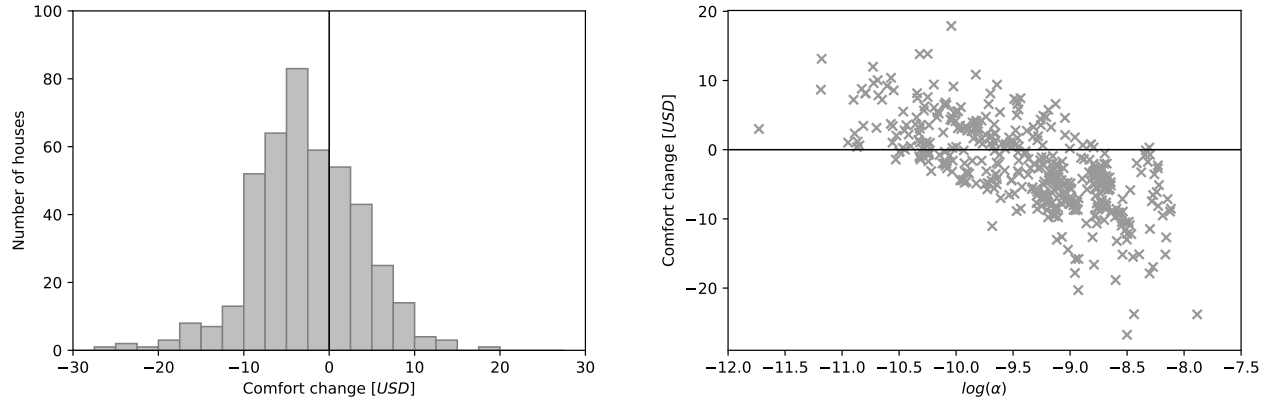
(a) Histogram of comfort changes by household

(b) House-wise comfort changes by comfort parameter

particularly negatively.

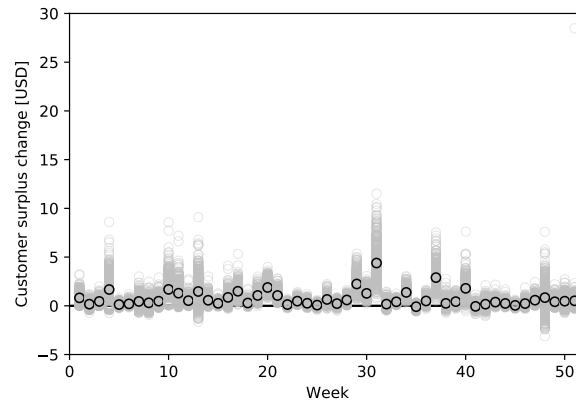Figure 13: Distribution of total consumer surplus changes

Fig. 13 further disentangles the consumer surplus changes for each week. Each grey circle represents an individual house during a specific week, the black circle represents the mean consumer surplus change. We find that changes differ throughout the year but can be high for some weeks and some customers. The minimum individual value within a week is -3.12 USD, the maximum value 28.48 USD.

	Dependent variable: Electricity bill savings	
	(1)	(2)
const	1.573	12.018***
	(1.043)	(2.151)
HVAC electricity costs	0.184***	0.173***
without DMS	(0.004)	(0.003)
share unresponsive load		0.277***
		(0.012)
correlation HVAC operation		-168.208***
and WS price		(25.300)
has gas heating		-5.867***
		(0.858)
Observations	437	437
R^2	0.794	0.923
Adjusted R^2	0.794	0.923
Residual Std. Error	7.683(df = 435)	4.707(df = 432)
F Statistic	1681.540*** (df = 1.0; 435.0)	1301.690*** (df = 4.0; 432.0)

Note:	*p<0.1; **p<0.05; ***p<0.01

Table 8: OLS regression results: Determinants of absolute electricity bill savings under demand management

Table 8 illustrates to which extent house-specific parameters explain the electricity bill savings when houses participate in demand management. We find that initial bills under a fixed retail rate explain 79% of the variance in savings, i.e. households which had large bills in the first place tend to save more. Additional significant factors are the share of unresponsive load, the correlation of HVAC dispatch and WS prices in the benchmark scenario, and the existence of an electric heating system.

	Dependent variable:		
	No DMS	DMS	DMS - No DMS
const	212541.519***	230608.946***	18067.427***
	(8127.562)	(8467.925)	(1329.597)
β	-202965.825***	-218175.761***	-15209.936***
	(8390.777)	(8742.162)	(1372.657)
γ_c	-1118.731***	-1336.657***	-217.926***
	(59.358)	(61.844)	(9.710)
γ_h	-717.890***	-833.158***	-115.268***
	(38.468)	(40.079)	(6.293)
Observations	292	292	292
R^2	0.817	0.845	0.828
Adjusted R^2	0.815	0.844	0.826
Residual Std. Error	1265.978	1318.994	207.103
	(df = 288)	(df = 288)	(df = 288)
F Statistic	427.499***	525.081***	460.894***
	(df = 3.0; 288.0)	(df = 3.0; 288.0)	(df = 3.0; 288.0)

Note:	*p<0.1; **p<0.05; ***p<0.01

Table 9: OLS regression results: Impact of energy efficiency measures on energy consumption

Table 9 illustrates to which extent the energy consumption of HVAC systems depends on the efficiency parameters of the house (houses with gas heating left out).

References

See references list in the main paper.